J. Cosmet. Sci., 71, 117–131 (May/June 2020)

Investigation of the Internal Structure of Human Hair with Atomic Force Microscopy

ROGER L. MCMULLEN and GUOJIN ZHANG, *Ashland Specialty Ingredients G.P., Bridgewater, New Jersey 08807 (R.L.M., G.Z.)*

Accepted for publication February 6, 2020.

Synopsis

The internal ultrafine structure of human hair was explored with atomic force microscopy (AFM). Cross sections of hair were prepared by a proprietary technique that provided a smooth surface for effective imaging in contact-mode AFM. Investigations of virgin hair revealed structural details of cortical and cuticle cells consistent with previous transmission electron microscopy (TEM) studies, in addition to the identification of a boundary region surrounding macrofibrils of the cortex. The effects of bleaching and solvent extraction on the internal structure of hair were also investigated. In the cuticle cell, bleaching causes the most damage to the endocuticle and cell membrane complex, evident by erosion of these components. Similarly, bleaching results in crevices, cracks, and asperities in the cortex of hair. In addition, the cortical cell membrane complex appears compromised along with either lipid or protein structures at the outer boundaries of macrofibrils. In delipidated hair, most structural components of the fiber appear intact with the exception of an overall swollen nature of the various morphological components.

INTRODUCTION

The ultrafine structure of human hair has captured the attention of scientists for decades. Most of what we currently know about hair morphology comes from a plethora of studies of thin sections of hair using transmission electron microscopy (TEM) (1–5). Despite advances made in our understanding of the hair structure, there still remain a number of unanswered questions about the physicochemical properties of hair. The advent of atomic force microscopy (AFM) techniques gave researchers an alternative route to explore the nanomechanical, nanotribological, and nanostructural properties of the hair fiber.

AFM studies of human hair started to appear in the literature in the late 1990s to early 2000s and mostly focused on the quantitative analysis of three-dimensional topographical images of the hair surface (6–8). A key advantage to using AFM as an investigative technique of the morphological properties of the hair fiber surface is that there is no need to coat the specimen with metal (e.g., gold and platinum) and studies can be conducted in ambient conditions (and even in solution) rather than vacuum (9). A study of cuticle

Address all correspondence to rmcmullen@ashland.com.
Current affiliation: Guojin Zhang, L'Oréal, Clark, New Jersey 07066.

step height and its swelling behavior in water as a function of pH was key to understanding possible access points to the fiber for cosmetic ingredients (7).

In addition to topographic imaging, one of the earliest AFM modes available to researchers was lateral force microscopy (LFM), also known as frictional force microscopy. In this technique, the lateral forces or twisting experienced by an AFM probe, as it moves from one side of a sample to the other, can be monitored. This mode of operation provided researchers with many insights into the nanotribology of the outer surface of hair, specifically the exposed surface of the cuticle. Early LFM studies sought to elucidate the role that free and covalently attached lipids play on the hair surface (10,11). In addition, AFM friction and adhesion mapping has also provided insight into the structural features of the lamellar layers of the cuticle. In any given area, the different cuticle layers (A layer, exocuticle, endocuticle, and inner layer) may be exposed to the surface and observed by AFM (12). Furthermore, the relationship between macro- and microscale friction of hair was investigated with LFM (13).

In another LFM study, it was suggested that stretching hair could possibly affect the nanotribological properties (coefficient of friction, adhesion, and surface roughness) of the hair surface (14). A rather modern approach for its time, Sadaie et al. (15) modified an AFM probe with a self-assembled monolayer and monitored the frictional interaction between the modified probe and the surface of hair, specifically probing the outermost 18-methyleicosanoic acid (18-MEA) layer of the cuticle. In fact, AFM has been an essential tool to demonstrate that 18-MEA plays a paramount role in the structural integrity of the cuticle (16).

AFM has also been at the forefront of allowing researchers to monitor intrinsic and extrinsic aging of hair. Intrinsic aging refers to the natural aging process of the fiber, and it has been shown by AFM that the surface roughness of hair increases with age, which is accompanied by a decline in the overall health state of the ultrafine morphological structures of hair (17). Extrinsic aging of hair refers to external elements that accelerate the aging process of hair, such as photodegradation or chemical treatments. Photodegradation leads to a substantial increase in the cuticle step height of hair and an increase in the size and depth of micropores apparent in the cuticle cell structure (18). The presence of micropores in the cuticle has been demonstrated by several techniques and their presence increases with photodegradation and bleaching (11,19). Using chemical force microscopy—achieved by chemically modifying AFM probes with $–CH_3$ and $–NH_2$ groups—allowed for the determination that bleaching of hair leads to the partial removal of the hydrophobic moiety—presumably 18-MEA—on the outermost surface of the cuticle (20).

Not surprisingly, great efforts have been made for understanding how AFM techniques could better be used to understand the deposition of cosmetic ingredients onto hair. Mostly, this includes monitoring the deposition of cationic ingredients onto the hair surface and performing frictional measurements with LFM (21–26). Although some ingredients decrease the dry friction of hair, it should be noted that application of cationic polymers to the hair normally increases the dry friction. In the wet state, however, cationic polymers reduce the capillary forces between the fibers and, as a result, lower the energy required to comb through the hair. Therefore, when conducting AFM measurements, a good understanding of the targeted state, dry or wet, and its relation to the application is needed.

Nanomechanical measurements of hair have also been carried out using AFM. Initial studies in this area included the determination of the mechanical properties (e.g.,

Young's modulus) of various lamellar constituents of the cuticle (27,28). Other studies focused on elucidating changes in the nanomechanical properties as a result of bleaching treatments or by changing the relative humidity. Not surprising, both bleaching and exposure to increasing levels of relative humidity reduce the modulus of the cuticle (29,30).

As technology in the field of AFM progresses, so does the analysis of hair by a variety of novel techniques. For example, surface potential imaging experiments—also known as Kelvin probe microscopy—were carried out to determine the electrostatic properties of the hair surface (31–34). Key findings from these studies shed light on the surface potential properties of the cuticle, in particular demonstrating the increased polar nature of the cuticle edge and also the influence of lipids on the wettability properties of the fiber (31,32). In addition, a nanoscale understanding of the electrostatic (static charging) properties of hair was also garnered with Kelvin probe microscopy (33,34).

Other important contributions by AFM technologies to understanding phenomena in hair include the use of nanoscale infrared spectroscopy and imaging for the high-resolution localization of structural lipids in hair (35). New insights have also been gained by attaching individual hair fibers to AFM probes and measuring the interaction between the probe fiber and another hair fiber (36,37). Furthermore, one of the caveats of any microscopy technique with human hair is the difficulty of monitoring the same region before and after treatment, which is circumvented with a practical mounting solution offered by Breakspear and Smith (38).

Almost all of the AFM studies investigating human hair have focused on probing the outer surface of the cuticle. From a different perspective—using torsional resonance mode AFM—researchers at Ohio State University analyzed cross sections and transverse sections of human hair (39,40). These studies shed light on some of the internal structures of hair, and the researchers were able to differentiate between the different sublamina of the cuticle and several features of the hair cortex. In this article, we demonstrate how a cross-sectioning technique in combination with contact-mode AFM allows us to visualize the various ultrafine structural components of the cuticle and cortex and investigate the influence of bleaching and delipidation on these structures.

MATERIALS AND METHODS

Studies were conducted on Asian hair purchased from International Hair Importers & Products Inc. (Glendale, NY). Before analysis, all hair was washed with a 3% (w/w) sodium laureth sulfate:cocamidopropyl betaine (12:2) mixture.

BLEACHING OF HAIR

Bleaching was carried out by mixing 120 g of Clairol Professional BW2 powder lightener (The Wella Corporation, Woodland Hills, CA) with 147 mL of Salon Care Professional 20 Volume Clear developer (Arcadia Beauty Labs LLC, Reno, NV). The resulting mixture was applied to damp hair for two 30-min intervals for a total bleaching time of 1 h. Bleached hair was shampooed twice with 3% (w/w) sodium laureth sulfate:cocamidopropyl betaine (12:2) before experiments.

DELIPIDATION OF HAIR

Using a Soxhlet extraction apparatus, free internal and surface lipids were removed from hair. This method is based on an established procedure in which hair is extracted with a series of solvents of increasing polarity (41). The apparatus consisted of a round-bottom flask to which a Soxhlet extraction tube was mounted. Inside the Soxhlet extraction tube, a bundle of hair was placed in a cellulose thimble. A condenser was mounted on top of the Soxhlet extraction tube. The effect of solvent extraction on hair was investigated first by treatment with *t*-butanol and *n*-hexane for 4 h each, then with a mixture of chloroform/methanol (70:30, v/v) for 6 h. In each procedure, 3 g of hair was treated with 250 mL of solvent in the Soxhlet extractor.

PREPARATION OF HAIR CROSS SECTIONS

Hair fibers were embedded in an epoxy resin block. The hair-epoxy block was cut into approximately 2-mm-thick sections. A Buehler MetaServ 250 Grinder-Polisher (Lake Bluff, IL) was used to prepare a smooth surface of the hair cross sections, suitable for AFM analysis. In this procedure, the hair-epoxy sections were sequentially grinded with aluminum oxide sandpaper with grit levels of 300, 600, and 1,200 with a head force set to 0.5 lb (≈2.22411 N). Both the head and plate rotate at a speed of 150 rpm in opposite directions. The lower head force and spin rate ensure mild abrasion and no tearing of the hair specimen. After sandpaper treatment, polish was applied with a liquid suspension of Al_2O_3 (0.05 μm). Suspended Al_2O_3 particles can roll and gently slide across the cloth and specimen. Finally, the hair-epoxy section was sonicated in deionized water for 1 min to eliminate the residues generated from grinding and polishing. This polishing technique was chosen as an alternative to conventional microtome preparation, which can introduce a variety of artifacts, including scores and tearing, chatters (thick and thin zones parallel to the knife edge), and compression artifacts. If performed incorrectly (e.g., with a large head force or high spinning speed), grinding and polishing can also introduce artifacts to the sample resulting in scratches, tearing, and uneven surfaces. Polishing is a preferential technique for preparing various biological specimens, such as bone or tooth, for microscopic investigations. Because a rough surface prevents the AFM probe from being able to raster effectively over the sample, the polishing technique creates a smooth surface and makes the sample more amenable for AFM analysis.

AFM MEASUREMENTS

Contact-mode AFM studies were carried out using a Multimode Nanoscope III (Bruker Corporation, Billerica, MA) using a 128-μm piezoelectric scanner. In this technique, a small tip attached to a cantilever is rastered in the *X* and *Y* directions on the surface of a sample, and the height (*Z* direction) is monitored. The operation of the instrument is based on the principal that a diode laser beam is focused on the top of a cantilever and reflected onto a position-sensitive photodetector. The probe (cantilever and tip) is shaped like a stylus, and as it traverses across the surface, the topographic features are mapped based on forces encountered between the probe and the sample. An Si_3N_4 probe (SNL-10) with a triangular cantilever (force constant of 0.06 N/m) from Bruker Corporation was used for all experiments. We operated the instrument in constant force mode, in which the

sample vertical height is continuously adjusted via an electronic feedback loop so that the probe maintains a constant force on the sample. All of the AFM micrographs presented in this article are raw images, which have not been filtered in any way, and are representative of many measurements carried out on each data set. AFM (and other microscopies) can sometimes be misleading because of the small region represented in an image. For this reason, we scout many areas to ensure that the selected images are representative of the data set. In the final analysis, at least three hair fiber cross sections were analyzed for each hair treatment set, and images were collected in a minimum of four sections of each cross section. It should be noted that care must be taken to ensure that enough fibers are sampled, and sufficient area of each fiber is analyzed to provide an accurate depiction of the morphological condition of the fiber. Each AFM image represents a small area of the hair fiber, and one can find a pristine or extremely damaged region on the same fiber.

RESULTS AND DISCUSSION

The evaluation of cross sections of hair is a novel technique that provides insight into the morphological properties of hair and the effects of damaging treatments and environmental exposure. We demonstrate the use of AFM analysis of hair cross sections to identify key structural components of the cuticle and cortex of hair while also offering insight into its structural architecture, in agreement with other recently published results. We also provide key insights into induced changes to the internal structural components of hair by hair bleaching, one of the most common chemical processes used in hair salons. In addition, we examine the effects of removing endogenous and exogenous lipids from hair and identify unique details that provide insight into the boundary region surrounding macrofibrils.

IDENTIFICATION OF ULTRAFINE STRUCTURAL FEATURES IN HAIR CROSS SECTIONS

Figure 1 contains an optical micrograph with an inset that roughly approximates the region of a hair cross section where the AFM micrograph was collected. Immediately apparent in

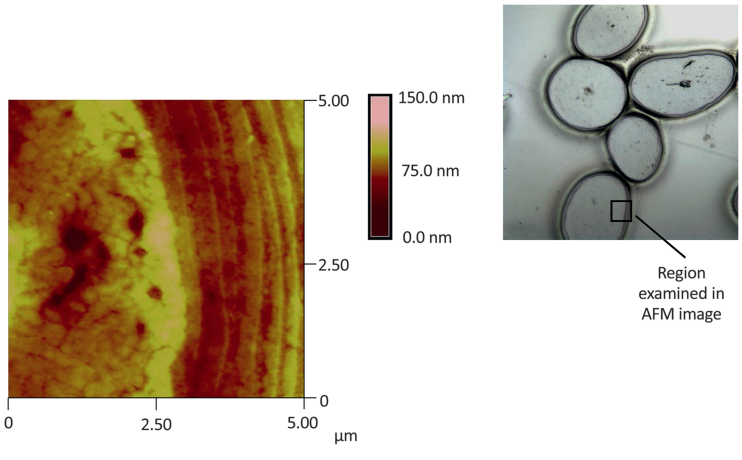

Figure 1. Typical AFM micrograph of a cross section of human hair. Note that only a section of the hair cross section is visible in the field of view of the image. The bright-field microscope image (reflection mode) of several cross sections of virgin hair is provided to give a scale of the section imaged by AFM.

the AFM image are the multiple layers of lamellar cuticle cells—roughly seven layers—surrounding the cortex of hair.

A magnified view of the cuticle cells is provided in Figure 2. Within the cuticle cells, density variations are observed in the image because of the different lamellar structures within each cuticle cell. Starting from the outside and going inward toward the cortex, each individual cuticle cell, or layer, consists of the following components with thickness indicated: A layer (110 nm), exocuticle (100–300 nm), endocuticle (50–300 nm), and inner layer (10–40 nm) (42).

Each cuticle cell is connected together by the cell membrane complex, which comprised a lipid layer on each side of the delta layer, known as the lower and upper layers, which are 2.5–4.0 nm thick. The delta layer is thought to serve as the intercellular cement between adjacent cuticle cells and believed to be composed mostly of polysaccharide. Overall, the cell membrane complex is roughly 25–28 nm thick (42). Some apparent features in the AFM micrograph of the cuticle cells are the various lamellar structures, which are outlined in the figure.

Several key features are evident when comparing the A layer, exocuticle, and endocuticle. Not surprisingly, the A layer, which is the mostly densely crosslinked sublamina structure in terms of cystine and isodipeptide crosslinks, is the least granular layer in the AFM micrograph of Figure 2. Roughly 30% of the amino acid composition of the A layer is cystine (ultrahigh sulfur protein) (43). The endocuticle, which is predominantly made of low–sulfur protein (*ca.* 3% cystine) content, is the most granular of the three layers. The exocuticle—the second most crosslinked sublamina of the cuticle (approximately 15–20% cystine content)—has a granular structure intermediate to that of the A layer and endocuticle. The cuticular cell membrane complex, located between each cuticle cell, is indicated by a very thin line in the image. It is more difficult to gain information about the cuticular cell membrane complex because of geometric constraints of the AFM tip. Initially, we contemplated the possibility that the granular structure of the cuticle was an artifact of the sample preparation technique. However, it should be noted that the granular

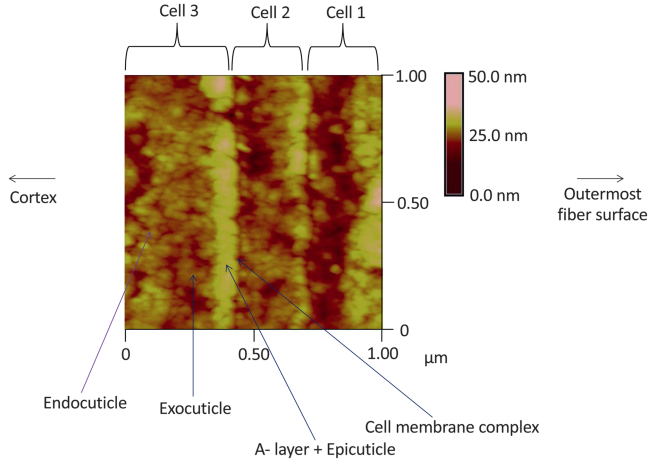

Figure 2. AFM micrograph of the cuticle region of a cross section of virgin hair. Three layers of cuticle cells can be discerned in the image where various morphological regions of the cuticle are indicated by the arrows.

structure observed for the cuticle was not found in the cortex region. Furthermore, the granular nature of the cuticle was proposed by Powell and Rogers to arise because of cysteine-rich granules from the cytoplasm that are fused together during the formation of the mature hair shaft (44).

The hair cortex is comprised of elongated cortical cells approximately 5 μm in diameter and 50 μm in length. The hierarchical appearance of the intermediate filaments can be described by envisioning two strands of slightly different keratin proteins arranged in an in-phase fashion and twisted together to produce a two-stranded rope (a coiled coil). Pairs of these associate to produce an antiparallel offset protein tetramer. By a process, the fine details of which remain to be elucidated, the tetramers associate both longitudinally and laterally to produce a discrete rod of semi-infinite length containing 32 protein chains in its transverse section. This is the "crystalline" part of the hair fiber known as the keratin intermediate filament (or microfibril). Hundreds of intermediate filaments are then embedded in a pseudo-hexagonal array within a cysteine-rich protein matrix (keratin associated proteins) to form the keratin macrofibril. Several tens of macrofibrils are packed longitudinally within each cortical cell. The macrofibrils are separated in places by other cellular components such as the effete cell nucleus, melanin pigment granules and, in places, a thin matrix of protein of low cysteine content (sometimes referred to as "non-keratin"). In a recent study, Kadir et al.(45) provided evidence that the amorphous matrix of hair contains granular structures ranging in size from 2 to 4 nm.

On close inspection of the cortex region in the AFM micrograph furnished in Figure 3, it is apparent that a number of intricate structures are present. The dark crater-like features (indicated by the white arrows), approximately 0.2–0.5 μm in diameter, more than likely are ghost melanin granules. Possibly, melanin granule structures were present in these locations, but during the hair cross section sample preparation procedure, these were sheared from the exposed surface. Previous studies report melanin granule dimensions on the order of 0.3–0.6 μm in width and 0.8–1.2 μm in length, which are in agreement with the ghost melanin granule measurements (46).

We are also able to discern cortical cell structures in Figure 3. These have varying forms and dimensions and are highlighted by the white circles in the micrograph. At times,

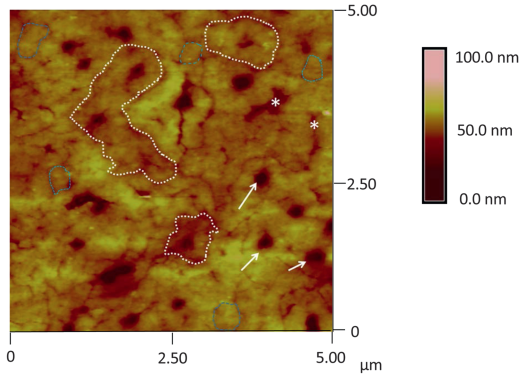

Figure 3. AFM micrograph of the cortical region of a cross section of virgin hair. The white arrows indicate places where melanin granules were present, whereas the white circles correspond to cortical cells. The smaller faint blue circles highlight the boundaries of several macrofibrils. It is suspected that nuclear remnants are also present (white asterisks).

cortical cells can have an irregular shape as illustrated in the figure. The small features in Figure 3, outlined in blue, correspond to macrofibrils. At a higher resolution, we can see the clear delineation between several macrofibrils (see Figure 4). Each macrofibril, measured to be approximately 400 nm in diameter, is surrounded by a thin boundary. It has been suggested in the past that there is a demarcation between adjacent macrofibrils denoted as intermacrofibrillar material (47).

Most reference texts report that the macrofibril dimensions for human hair typically range from 40 to 500 nm in diameter (43,48,49). In wool, there are three types of cortical cells: paracortical, orthocortical, and mesocortical cells. In human hair, researchers have used terminology such as ortho-type and para-type cortical cells to denote the similarity of cell types that share some common features with those from wool. The size and structure of macrofibrils in wool are fairly consistent for each cell type. However, the macrofibrils in human hair were reported to vary considerably in size and shape (50). Therefore, it should come of no surprise that there is such high variability in the size of macrofibrils reported from various sources. Regardless, our measured values (approximately 400 nm) appear to be in line with those previously reported in the literature. Noteworthy, in a study carried out by Harland et al., (47) the thickness of the cross section was found to cause some variability in the measurement of macrofibrillar dimensions because of the tilt angle of intermediate filaments.

Another key feature of hair morphology is the medulla. It is not always present in hair fibers and is most commonly found in hair of Asian descent. For example, in Caucasian hair, the medulla is not continuous along the length of the fiber, so depending on the location from which the fiber cross section is obtained, you may or may not observe the medulla structure. Regardless, Figure 5 contains an AFM image of the cross section of hair containing a medulla. In agreement with previous studies, the medulla appears as a porous and rough structure (51).

Historically, not that much attention was given to understanding the structure and function of the medulla. It was merely thought to be a vacuolated morphological component of the fiber. Studies in recent years, however, have shown that it is rich in lipids and also contain fibrillar protein structures (35,51,52). Furthermore, studies have demonstrated that the medulla is a fairly complex structure and consists of a medullary tube surrounded by two types of medullary cells and vesicles with proteinaceous granules (53).

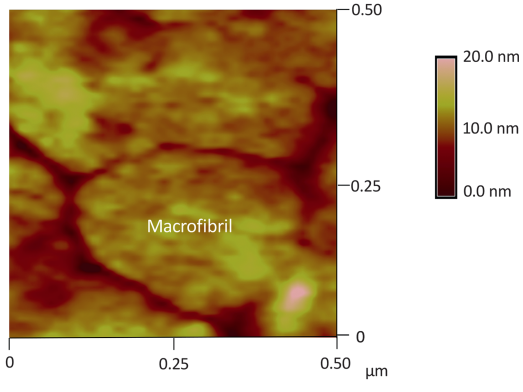

Figure 4. AFM micrograph of a magnified section of the region shown in Figure 3. The slightly elliptically shaped feature in the center of the image is a macrofibril.

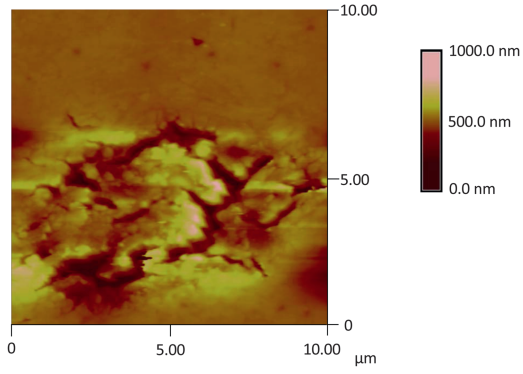

Figure 5. AFM micrograph of the medulla region of virgin hair illustrating its rough and porous nature.

EFFECT OF BLEACHING ON HAIR MORPHOLOGY

Hair bleaching is a common cosmetic procedure that is used to introduce highlights to the hair. A typical bleaching formulation contains a two-part system; the first is the bleaching powder, which contains persulfate salts that accelerate the bleaching process, whereas the second is typically a developer and contains H_2O_2. The ultimate goal of this procedure is the destruction of melanin granules; however, it results in a number of other secondary effects resulting in damage to the hair fiber. Such damage is manifested in changes to the surface properties of hair, as monitored by surface techniques such as combing force and surface tension measurements, as well as damage to the internal components of the fiber, which can be followed by tensile strength and differential scanning calorimetry measurements of hair (54,55). At the chemical level, one of the hallmarks of hair bleaching is the breakdown of disulfide bonds, resulting in the formation of cysteic acid residues (56,57). In addition, the lipid structures in hair are also vulnerable to the bleaching process (58).

Figure 6 contains an AFM image of a cross section of the cuticle region of bleached hair. Three cuticle cells can be discerned in the micrograph. A comparison should be made

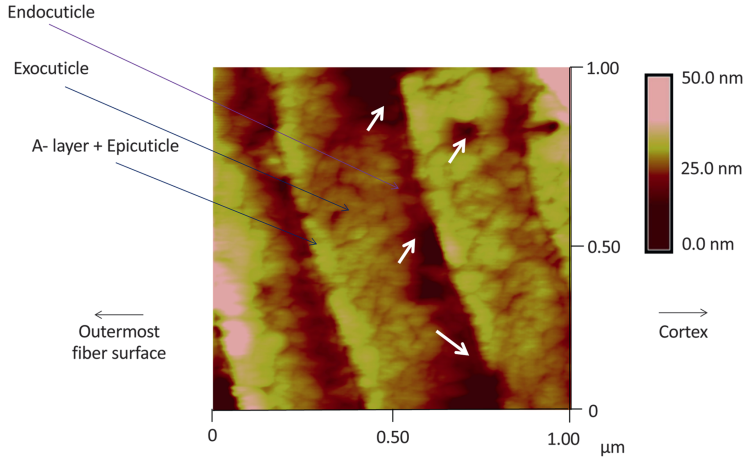

Figure 6. AFM micrograph of the cuticle of bleached hair. In the image of the cuticle, the white arrows indicate regions of the cuticle where severe damage has been induced in the cell membrane complex and endocuticle.

with the corresponding image of the cuticle of virgin hair in Figure 2. Structurally, the most noticeable difference between the virgin and bleached hair is the appearance of dark voids that are especially evident in the endocuticle region. Because the endocuticle has the lowest density of crosslinking of the sublamina layers, it seems likely that this would be the region most susceptible to damage from the bleaching procedure. There are also voids in the cuticle of the virgin fiber (Figure 2); however, they are not nearly as large or deep as those found in bleached hair. These findings are in agreement with TEM studies where it was shown that the electron density of the endocuticle of bleached hair—fixed with osmium tetroxide and stained with uranium acetate and lead acetate—was greater than that of virgin hair, more so than the other lamellar structures (59).

An AFM micrograph of the cortex of bleached hair is provided in Figure 7. Immediately apparent in the image are the large amounts of cracks, crevices, and other asperities in the bleached hair cross section (compare with virgin hair shown in Figure 3). Focusing in on the cortex at greater resolution allows us to discern the macrofibrillar structures and to make a comparison between virgin and bleached hair (Figure 8). In the bleached sample, there appears to be an erosion of biomaterial at the outer edges of the macrofibrils. This could suggest the presence of a low-sulfur–containing protein more susceptible to degradation by bleaching than the inner core of the macrofibril, or the possibility that a cell membrane-like material could be present on the exterior of the macrofibril and then removed by the bleaching procedure. It should also be pointed out that, regardless of the material, erosion would be expected to proceed from the exposed edges inward.

We did not observe noticeable differences in the medulla region of bleached hair as compared with virgin hair. This is surprising because previous studies demonstrated greater quantities of lipids in the medulla than other regions of the fiber (52). Removal of lipids by bleaching and other chemical processes could result in a change in the morphological appearance of the medulla, although this requires further investigation.

INVESTIGATION OF DELIPIDATED HAIR

Hair contains a variety of lipids that consist of free fatty acids, cholesterol, ceramides, cholesterol esters, and cholesterol sulphate (60). Typically, hair lipids are categorized as

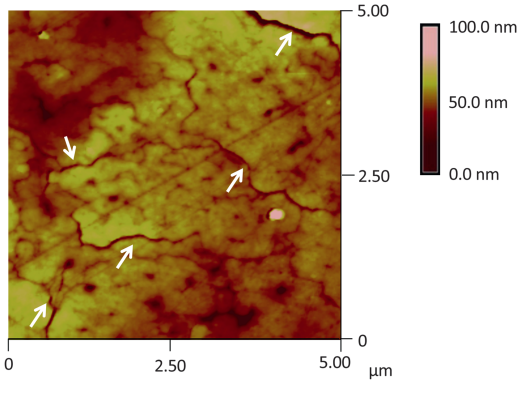

Figure 7. AFM micrograph of the cortex of bleached hair. The arrows in the image of the cortex point to major cracks and crevices within the cortical structure caused by the bleaching procedure.

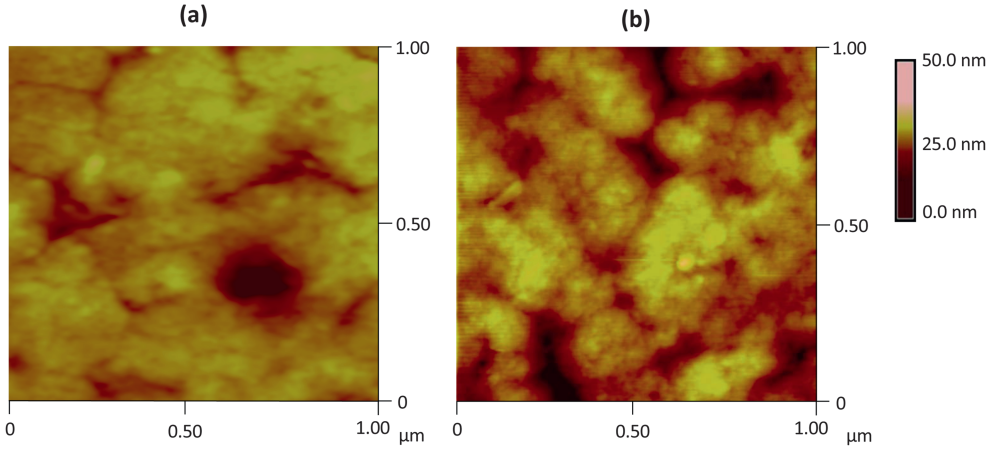

Figure 8. AFM micrographs of the cortex of (A) virgin hair and (B) bleached hair.

endogenous or exogenous. Endogenous lipids carry out a structural function, serving as the building blocks of the cell membrane complex in hair. Compositionally and structurally, there are three different types of cell membrane complex in hair fibers: (i) cuticle cell membrane complex situated above and below each cuticle cell, (ii) cortex cell membrane complex that surrounds each spindle-shaped cortical cell, and (iii) cuticle–cortex cell membrane complex that provides the boundary between the cuticle and cortex (61). Exogenous lipids arise from the sebaceous gland, which coats the exterior of the fiber and also secretes lipids within the fiber structure.

The Soxhlet extraction method used in this study more than likely removes both endogenous and exogenous lipids leaving only covalently bound 18-MEA, which is present in the outermost layer of each cuticle cell. Figure 9 contains an AFM micrograph of the cuticle of delipidated hair. It appears there is a greater degree of demarcation between cuticle cells than the virgin hair (see Figure 2). In addition, the cells adopt a swollen appearance—similar to that found in an earlier TEM study by Takizawa et al. (62) in permanent waved hair. The density of the various lamellar structures is less distinct in the delipidated hair than virgin and bleached hair. Overall, there appears to be a less granular

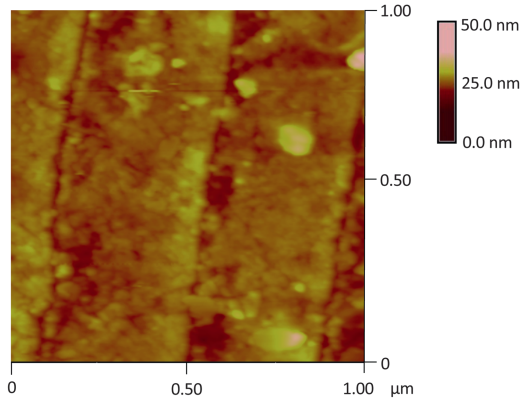

Figure 9. AFM micrograph of the cortical region of delipidated hair.

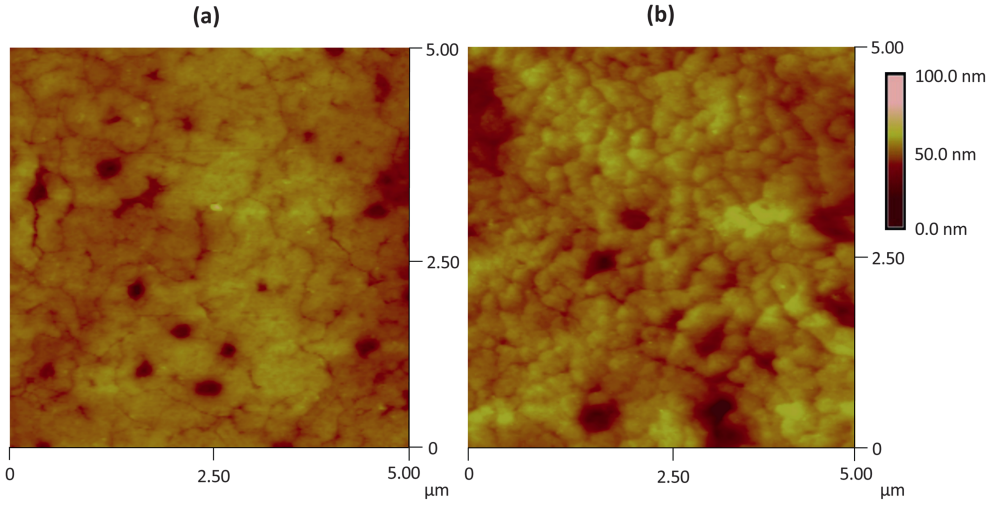

Figure 10. AFM micrographs of the cortical region of (A) virgin and (B) delipidated hair.

appearance of the cuticle components. Again, swelling of the components in the cuticle cells due to solvent extraction could account for such an observation; however, we should not discount the possibility that the effects of the grinding and polishing procedure used in this study could also lead to the granular appearance of the morphological components of hair as observed in Figures 2 and 6. However, this is unlikely as the granular structure is not observed in the cortex of hair.

An AFM micrograph of the cortex of virgin and delipidated hair is provided in Figure 10. As compared with virgin hair, the image of delipidated hair clearly shows a delineation surrounding the macrofibrils. Possibly, such a result suggests that intermacrofibrillar material or lipids surrounding the macrofibrils are removed during the lipid extraction procedure. Similar to the features observed in Figure 1, the small pits seen as dark spots in the images, presumably correspond to sites where melanin granules were present, but then removed during the polishing step of the sample preparation procedure. Another interesting feature in the cortex of delipidated hair is the swollen nature of the macrofibrils. Such a finding suggests that extraction of hair with solvents alters the structural morphology of the macrofibrils, although earlier work using the same extraction technique as used in this report demonstrated that solvent extraction had no effect on the structural integrity of keratin intermediate filaments as measured by differential scanning calorimetry (52). In TEM studies, the swollen nature of the macrofibrils in thioglycolic acid–treated wool/hair was also found and attributed to the reduction of disulfide bonds followed by reaction of osmium tetroxide with the sulfhydryl groups (1,62). The fact that this phenomenon also occurs in solvent-treated hair leads one to inquire about the source of the swelling behavior.

CONCLUSIONS

In this study, we demonstrate the use of cross-sectional analysis of human hair fibers by AFM. The ultrafine structure of hair was delineated—confirming previous work with

TEM—and new insights about the intermacrofibrillar region were introduced. Comparisons were made between virgin and bleached hair as well as delipidated hair. In the hair cuticle, damage to the fiber is especially noticeable in the endocuticle and is manifested in the form of low-density regions that likely correspond to disintegration of structural proteins. The cortical cells of bleached hair contain crevices, cracks, and cavities as a result of the destructive bleaching procedure. Likewise, the intermacrofibrillar material is also degraded. In delipidated hair, the morphological components of hair (i.e., cuticle lamellar structures and macrofibrils) become swollen. In the past, such behavior was also observed in hair prepared for TEM studies and attributed to the reaction of osmium tetroxide (biological staining agent) with sulfhydryl groups of chemically reduced keratin fibers. We are left to question the real source of swelling, which might be related to lipid structures in the fiber or the effects of solvent extraction on protein structure.

REFERENCES

(1) G. Rogers, Electron microscopy of wool, *J. Ultrastruct. Res.*, **2**(3), 309–330 (1959).
(2) J. Swift, The electron histochemistry of cystine—containing proteins in thin transverse sections of human hair, *J. Roy. Microsc. Soc.*, **88**(4), 449–460 (1968).
(3) M. Birbeck and E. Mercer, The electron microscopy of the human hair follicle. Part 1. Introduction and the hair cortex, *J. Biophys. Biochem. Cytol.*, **3**(2), 203–214 (1957).
(4) M. Birbeck and E. Mercer, The electron microscopy of the human hair follicle. Part 2. The hair cuticle, *J. Biophys. Biochem. Cytol.*, **3**(2), 215–222 (1957).
(5) M. Birbeck and E. Mercer, The electron microscopy of the human hair follicle. Part 3. The inner root sheath and trichohyaline, *J. Biophys. Biochem. Cytol.*, **3**(2), 223–230 (1957).
(6) S. Gurden, V. Monteiro, E. Longo, and M. Ferreira, Quantitative analysis and classification of AFM images of human hair, *J. Microsc.*, **215**(1), 13–23 (2004).
(7) H. You and L. Yu, Atomic force microscopy as a tool for study of human hair, *Scanning*, **19**(6), 431–437 (2006).
(8) J. Smith, A quantitative method for analysing AFM images of the outer surfaces of human hair, *J. Microsc.*, **191**(Pt 3), 223–228 (1998).
(9) G. Poletti, F. Orsini, C. Lenardi, and E. Barborini, A comparative study between AFM and SEM imaging on human scalp hair, *J. Microsc.*, **211**(3), 249–255 (2003).
(10) S. Breakspear, J. Smith, and G. Luengo, Effect of the covalently linked fatty acid 18-MEA on the nanotribology of hair's outermost surface, *J. Struct. Biol.*, **149**(3), 235–242 (2005).
(11) R. McMullen and S. Kelty, Investigation of human hair fibers using lateral force microscopy, *Scanning*, **23**(5), 337–345 (2001).
(12) J. Smith, J. Tsibouklis, T. Nevell, and S. Breakspear, AFM friction and adhesion mapping of the substructures of human hair cuticles, *Appl. Surf. Sci.*, **285**(Pt B), 638–644 (2013).
(13) C. LaTorre and B. Bhushan, Investigation of scale effects and directionality dependence on friction and adhesion of human hair using AFM and macroscale friction test apparatus, *Ultramicroscopy*, **106**(8), 720–734 (2006).
(14) T. Chen, H. Liu, and W. Yu, Investigation of nanotribological characterization of stretched European hair using atomic force microscopy, *Adv. Mater. Res.*, **821–822**, 274–277 (2013).
(15) M. Sadaie, N. Nishikawa, S. Ohnishi, K. Tamada, K. Yase, and M. Hara, Studies of human hair by friction force microscopy with the hair-model-probe, *Colloids Surf. B Biointerfaces*, **51**(2), 120–129 (2006).
(16) J. Smith and J. Swift, Maple syrup urine disease hair reveals the importance of 18-methyleicosanoic acid in cuticular delamination, *Micron*, **36**(3), 261–266 (2005).
(17) K. Jeong, K. Kim, G. Lee, S. Choi, T. Jeong, M. Shin, H. Park, W. Sim, and M. Lee, Investigation of aging effects in human hair using atomic force microscopy, *Skin Res. Technol.*, **17**(1), 63–68 (2011).
(18) M. Richena and C. Rezende, Effect of photodamage on the outermost cuticle layer of human hair, *J. Photochem. Photobiol. B Biol.*, **153**, 296–304 (2015).
(19) Y. Hessefort, B. Holland, and R. Cloud, True porosity measurement of hair: a new way to study hair damage mechanisms, *J. Cosmet. Sci.*, **59**(4), 303–315 (2008).

(20) M. Korte, S. Akari, H. Kühn, N. Baghdadli, H. Möhwald, and G. Luengo, Distribution and localization of hydrophobic and ionic chemical groups at the surface of bleached human hair fibers. *Langmuir*, **30**(41), 12124–12129 (2014).
(21) C. LaTorre and B. Bhushan, Nanotribological effects of hair care products and environment on human hair using atomic force microscopy, *J. Vac. Sci. Technol.*, **23**(4), 1034–1045 (2005).
(22) S. Lee, S. Zürcher, A. Dorcier, G. Luengo, and N. Spencer, Adsorption and lubricating properties of poly(l-lysine)-graft-poly(ethylene glycol) on human-hair surfaces, *ACS Appl. Mater. Interfaces*, **1**(9), 1938–1945 (2009).
(23) R. Lodge and B. Bhushan, Surface characterization of human hair using tapping mode atomic force microscopy and measurement of conditioner thickness distribution, *J. Vac. Sci. Technol.*, **24**(4), 1258–1269 (2006).
(24) V. Monteiro, A. Natal, L. Soledade, and L. Longo, Morphological analysis of polymers on hair fibers by SEM and AFM, *Mat Res.*, **6**(4), 501–506 (2003).
(25) A. Pfau, P. Hössel, S. Vogt, R. Sander, and W. Schrepp, The interaction of cationic polymers with human hair, *Macromol. Symp.*, **126**(1), 241–252 (2011).
(26) C. Durkan and N. Wang, Nanometre-scale investigations by atomic force microscopy into the effect of different treatments on the surface structure of hair, *Int. J. Cosmet. Sci.*, **36**(6), 598–605 (2014).
(27) A. Parbhu, W. Bryson, and R. Lal, Disulfide bonds in the outer layer of keratin fibers confer higher mechanical rigidity: correlative nano-indentation and elasticity measurement with an AFM, *Biochem.*, **38**(36), 11755–11761 (1999).
(28) J. Smith and J. Swift, Lamellar subcomponents of the cuticular cell membrane complex of mammalian keratin fibres show friction and hardness contrast by AFM, *J. Microsc.*, **206**(3), 182–193 (2002).
(29) B. Bhushan and N. Chen, AFM studies of environmental effects on nanomechanical properties and cellular structure of human hair, *Ultramicroscopy*, **106**(8), 755–764 (2006).
(30) C. Clifford, N. Sano, P. Doyle, and M. Seah, Nanomechanical measurements of hair as an example of microfibre analysis using atomic force microscopy nanoindentation, *Ultramicroscopy*, **114**:38–45 (2012).
(31) V. Dupres, T. Camesano, D. Langevin, A. Checco, and P. Guenoun, Atomic force microscopy imaging of hair: correlations between surface potential and wetting at the nanometer scale, *J. Colloid Interface Sci.*, **269**(2), 329–335 (2004).
(32) V. Dupres, D. Langevin, P. Guenoun, A. Checco, G. Luengo, and F. Leroy, Wetting and electrical properties of the human hair surface: delipidation observed at the nanoscale, *J. Colloid Interface Sci.*, **306**(1), 34–40 (2007).
(33) R. Lodge and B. Bhushan, Effect of physical wear and triboelectric interaction on surface charge as measured by Kelvin probe microscopy, *J. Colloid Interface Sci.*, **310**(1), 321–330 (2007).
(34) I. Seshadri and B. Bhushan, Effect of rubbing load on nanoscale charging characteristics of human hair characterized by AFM based Kelvin probe, *J. Colloid Interface Sci.*, **325**(2), 580–587 (2008).
(35) C. Marcott, M. Lo, K. Kjoller, F. Fiat, N. Baghdadli, G. Balooch, and G. Luengo, Localization of human hair structural lipids using nanoscale infrared spectroscopy and imaging, *Appl. Spectrosc.*, **68**(5), 564–569 (2014).
(36) E. Max, W. Häfner, F. Wilco Bartels, A. Sugiharto, C. Wood, and A. Fery, A novel AFM based method for force measurements between individual hair strands, *Ultramicroscopy*, **110**(4), 320–324 (2010).
(37) H. Mizuno, G. Luengo, and M. Rutland, New insight on the friction of natural fibers. Effect of sliding angle and anisotropic surface topography, *Langmuir*, **29**(19), 5857–5862 (2013).
(38) S. Breakspear and J. Smith, Returning to the same area of hair surfaces before and after treatment: a longitudinal AFM technique, *J. Microsc.*, **215**(1), 34–39 (2004).
(39) B. Bhushan, Nanoscale characterization of human hair and hair conditioners, *Prog. Mater. Sci.*, **53**(4), 585–710 (2008).
(40) N. Chen and B. Bhushan, Morphological, nanomechanical and cellular structural characterization of human hair and conditioner distribution using torsional resonance mode with an atomic force microscope, *J. Microsc.*, **220**(2), 96–112 (2005).
(41) P. Wertz and D. Downing, Integral lipids of mammalian hair, *Comp. Biochem. Physiol.*, **92B**(4), 759–761 (1989).
(42) J. Swift, Human hair cuticle: biologically conspired to the owner's advantage, *J. Cosmet. Sci.*, **50**(1), 23–47 (1999).
(43) C. Robbins, *Chemical and Physical Behavior of Human Hair* (Springer, Heidelberg), 2012.
(44) B. Powell and G. Rogers, The role of keratin proteins and their genes in the growth, structure and properties of hair, in *Formation and Structure of Human Hair*, P. Jollès, H. Zahn, and H. Höcker. Eds. (Birkhäuser Verlag, Basel, 1997), pp. 59–148.

(45) M. Kadir, X. Wang, B. Zhu, J. Liu, D. Harland, and C. Popescu, The structure of the "amorphous" matrix of keratins, *J. Struct. Biol.*, **198**(2), 116–123 (2017).
(46) P. Prem, K. Dube, S. Madison, and J. Bartalone, New insights into the physicochemical effects of ammonia/peroxide bleaching of hair and sepia melanins, *J. Cosmet. Sci.*, **54**(4), 395–409 (2003).
(47) D. Harland, R. Walls, J. Vernon, J. Dyer, J. Woods, and F. Bell, Three-dimensional architecture of macrofibrils in the human scalp hair cortex, *J. Struct. Biol.*, **185**(3), 397–404 (2014).
(48) M. Feughelman, Morphology and properties of hair, in *Hair and Hair Care. Cosmetic Science and Technology*, D. Johnson. Ed. (Marcel Dekker, New York, 1997), Vol. 17, pp. 1–12.
(49) J. Swift, The structure and chemistry of human hair, in *Practical Modern Hair Science*, T. Evans and R. Wickett, Eds. (Allured, Carol Stream, IL, 2012), pp. 1–37.
(50) W. Bryson, D. Harland, J. Caldwell, J. Vernon, R. Walls, J. Woods, S. Nagase, T. Itou, and K. Koike, Cortical cell types and intermediate filament arrangements correlate with fiber curvature in Japanese human hair, *J. Struct. Biol.*, **166**(1), 46–58 (2009).
(51) R. De Cássia Comis Wagner, P. Kunihiko Kiyohara, M. Silveira, and I. Joekes, Electron microscopic observations of human hair medulla, *J. Microsc.*, **226**(1), 54–63 (2007).
(52) R. McMullen, D. Laura, S. Chen, D. Koelmel, G. Zhang, and T. Gillece, Determination of physicochemical properties of delipidized hair, *J. Cosmet. Sci.*, **64**(5), 355–370 (2013).
(53) A. Yamauchi and K. Yamauchi, New aspects of the structure of human scalp hair-II: tubular structure and material flow property of the medulla, *J. Cosmet. Sci.*, **69**(1), 19–33 (2018).
(54) C. Kunchi, K. Venkateshan, N. Reddy, and R. Adusumalli, Correlation between mechanical and thermal properties of human hair, *Int. J. Trichol.*, **10**(5), 204–210 (2018).
(55) A. Vaynberg, M. Stuart, and X. Wu, Differential wetting characterization of hair fibers, *J. Cosmet. Sci.*, **61**(1), 33–41 (2012).
(56) K. Suzuta, K. Watanabe, T. Maeda, and L. Ito, Evaluation of cysteic acid in bleached hair using infrared spectroscopy, *J. Fiber Sci Technol.*, **72**(1), 1–8 (2016).
(57) A. Grosvenor, S. Deb-Choudhury, P. Middlewood, A. Thomas, E. Lee, J. Vernon, J. Woods, C. Taylor, F. Bell, and S. Clerens, The physical and chemical disruption of human hair after bleaching – studies by transmission electron microscopy and redox proteomics, *Int. J. Cosmet. Sci.*, **40**(6), 536–548 (2018).
(58) K. Joo, A. Kim, S. Kim, B. Kim, H. Lee, S. Bae, J. Lee, and K. Lim, Metabolomic analysis of amino acids and lipids in human hair altered by dyeing, perming and bleaching, *Exp. Dermatol.*, **25**(9), 729–731 (2016).
(59) T. Imai, The influence of hair bleach on the ultrastructure of human hair with special reference to hair damage, *Okajimas Folia Anat. Jpn.*, **88**(1), 1–9 (2011).
(60) M. Martí, C. Barba, A. Manich, L. Rubio, C. Alonso, and L. Coderch, The influence of hair lipids in ethnic hair properties, *Int. J. Cosmet. Sci.*, **38**(1), 77–84 (2015).
(61) C. Robbins, The cell membrane complex: three related but different cellular cohesion components of mammalian hair fibers, *J. Cosmet. Sci.*, **60**(4), 437–465 (2009).
(62) T. Takizawa, T. Takizawa, S. Arai, M. Osumi, and T. Saito, Ultrastructure of human scalp hair shafts as revealed by freeze-substitution fixation, *Anat. Rec.*, **251**(3), 406–413 (1998).